International Journal of Heat and Mass Transfer 52 (2009) 2289–2299

Contents lists available at ScienceDirect

International Journal of Heat and Mass Transfer

journal homepage: www.elsevier.com/locate/ijhmt

Sintered porous heat sink for cooling of high-powered microprocessors for server applications

Randeep Singh [a,*], Aliakbar Akbarzadeh [a], Masataka Mochizuki [b]

[a] Energy Conservation and Renewable Energy Group, School of Aerospace, Mechanical and Manufacturing Engineering, RMIT University, P.O. Box 71, Bundoora East Campus, Bundoora, Vic. 3083, Australia
[b] Thermal Technology Division, R&D Dept., Fujikura Ltd., 1-5-1, Kiba, Koto-Ku, Tokyo 135-8512, Japan

ARTICLE INFO

Article history:
Received 12 February 2008
Received in revised form 22 November 2008
Available online 12 January 2009

Keywords:
Sintered porous heat sink
Liquid cooling
Thermal control
Porous structure
Computer cooling

ABSTRACT

This paper experimentally investigates the sintered porous heat sink for the cooling of the high-powered compact microprocessors for server applications. Heat sink cold plate consisted of rectangular channel with sintered porous copper insert of 40% porosity and 1.44×10^{-11} m^2 permeability. Forced convection heat transfer and pressure drop through the porous structure were studied at Re $\leqslant$ 408 with water as the coolant medium. In the study, heat fluxes of up to 2.9 MW/m^2 were successfully removed at the source with the coolant pressure drop of 34 kPa across the porous sample while maintaining the heater junction temperature below the permissible limit of 100 ± 5 °C for chipsets. The minimum value of 0.48 °C/W for cold plate thermal resistance (R_{cp}) was achieved at maximum flow rate of 4.2 cm^3/s in the experiment. For the designed heat sink, different components of the cold plate thermal resistance (R_{cp}) from the thermal footprint of source to the coolant were identified and it was found that contact resistance at the interface of source and cold plate makes up 44% of R_{cp} and proved to be the main component. Convection resistance from heated channel wall with porous insert to coolant accounts for 37% of the R_{cp}. With forced convection of water at Re = 408 through porous copper media, maximum values of 20 kW/m^2 K for heat transfer coefficient and 126 for Nusselt number were recorded. The measured effective thermal conductivity of the water saturated porous copper was as high as 32 W/m K that supported the superior heat augmentation characteristics of the copper–water based sintered porous heat sink. The present investigation helps to classify the sintered porous heat sink as a potential thermal management device for high-end microprocessors.

1. Introduction

Cooling of electronic devices is very critical to promote runtime reliability, optimal performance and extended operational life span of the product. At present, thermal management of power electronics in high-end workstations, application servers and data centers [1,2] is an exceedingly demanding area that requires continuous research efforts to develop efficient and cost competitive cooling solutions. Typically, the waste heat output by the high density microprocessors or Central Processing Unit (CPU) can be as high as 150–250 W [3,4] and is expected to show future rise with the increase in processor clock speed and inclusion of advanced computing capabilities. As a result, at the high end of the power spectrum and for a thermal footprint of 1 cm^2, these chips can produce ultrahigh heat fluxes of 2.5 MW/m^2. At chip level, such power densities, if not handled adequately, present problems related to elevated die temperatures, local hot spots, low performance and even component malfunctioning. At system level, the total heat dumped by the equipment into the computer room or data center goes up that increases the demand on the computer room air conditioning (CRAC) and thus overall cooling cost. At present, the heat dissipated by a 2 foot (60.96 cm) by 2½ foot (76.2 cm) rack can be 10 kW (~22,000 W/m^2) or higher and the design for the future equipments assume 30–50 kW (~65,000–108,000 W/m^2) heat load in the same space [1]. At room level, the current power densities for the data center room is 500–2000 W/m^2 and are projected to jump beyond 3000 W/m^2 in the near future [5]. It is evident that future forecasts for the heat fluxes based on die, product and room footprint are strikingly high. Therefore, technological improvements in the cooling of high density microprocessors for the servers are necessary for the effective thermal management of mission critical electronics in data centers.

Chip level thermal management of data centers using direct liquid cooling of microprocessors can provide one of the most viable thermal control solution and offer incentives on performance and cost of the next generation high-end data centers. In essence, liquid based cooling systems are single phase heat transfer

* Corresponding author. Tel.: +61 3 9925 6024; fax: +61 3 9925 6108.
E-mail address: randeep.singh@rmit.edu.au (R. Singh).

0017-9310/$ - see front matter © 2008 Elsevier Ltd. All rights reserved.
doi:10.1016/j.ijheatmasstransfer.2008.11.016

Nomenclature

A	area, m^2
h	heat transfer coefficient, W/m^2 K
k	thermal conductivity, W/m K
k_p	specific permeability of the porous medium, m^2
$\dot{m}$	mass flow rate, kg/s
$\dot{Q}$	heat load, W
R	thermal resistance, °C/W
T	temperature, °C
t	thickness, m
$\dot{V}$	volume flow rate, m^3/s
W_{pump}	pumping power, W
ΔP	pressure drop, Pa

Greek symbols

μ	viscosity, Pa s
ε	porosity, %

Constants

α	0.59 (as in Eq. (10))

Subscripts

a	applied
az	active zone of cold plate
b	base of the cold plate
bf	bottom face
cp	cold plate
ct	contact
cu	copper
conv	convective
e	effective
ew	external wall
fi	fluid inlet
fm	fluid mean
fo	fluid outlet
h	heater
iw	internal wall
j	junction
l	liquid
o	overall
p	porous structure
s	saturated porous structure
sp	spreading
tf	top face
TIM	thermal interface material
w	wall
x	cross section

modules that utilises sensible heat capacity of the liquid medium flowing under actively pumped means to transport heat from the source to remotely located heat sink. It should be noted that liquid cooling is much more effective than air cooling to remove heat locally at the source due to the superior heat transfer characteristics of liquid including specific heat capacity, heat transfer coefficient and thermal conductivity. In a liquid cooling unit, cold plate is a critical design element that dictates the overall performance of the unit and is required to spread, acquire and transfer heat from the source to the working fluid.

Cold plate technology based on the porous structure provides an effective and capable candidate for the thermal management of electronic devices [6]. Here, the capability of the porous media to increase the surface area in contact with the coolant and to intensify the fluid flow mixing helps to enhance the convective heat transfer between the fluid and the porous matrix. Trends towards miniaturization in future electronics needs parallel development in the cooling modules. Porous media provide twofold advantages when compared to the microchannel or finned structures. Firstly, the porous heat sink offers very high contact surface area to volume ratio that helps to contain them in limited available space as well as provide large heat transfer area. Secondly, the bulk of porous matrix consists of networks of interconnected microchannels with torturous flow path which provides high velocity turbulent mixing of the fluid and thus high heat transfer coefficient. Porous heat sinks made from metal foams, packed beds and sintered metal powders have been extensively used for electronic cooling applications.

Metal foam heat sinks fabricated from aluminum, carbon and silicon carbide have been used with air or water as coolant medium under forced convection [7–10]. Hsieh et al. [11] performed an experimental investigation on the effects of porosity, pore density and fluid velocity on the heat transfer characteristics of aluminum foam heat sink under forced convective cooling conditions using air as the coolant. Results showed that the Nusselt number increased with increasing pore density and porosity of the aluminum foam, due to the fact that the heat transfer area of the foam increases as pore density and porosity increase. It was also noted that the temperature difference between the solid and the gas phases decreased with the increase of the Reynolds number of the air flow and increase in the porosity and pore density of the aluminum foam. Lee et al. [12] demonstrated cooling of 1 cm^2 chip with 100 W power output using aluminum metal foam heat sink. Chao and Li [13] reported significant improvement in the power dissipation from a Ball Grid Array (BGA) when a pin-fin sink was replaced with an aluminum–foam heat sink under forced convection conditions. In spite of excellent thermal performance of metal foams reported in the literature, porous heat sinks based on the metal powder provides more compact design, i.e. larger surface area and better effective thermal conductivity than the foams structures [14].

For the purpose of electronics cooling, convective heat and mass transfer in porous medium based on non-sintered or sintered metal power has been widely studied by researchers worldwide. In theoretical and numerical investigation, models based on local thermal equilibrium or local thermal non-equilibrium has been used for the energy equation. Jeng et al. [15] presented an algorithm model based on the fin theory and the concept of the thermal network for estimating the forced convection heat transfer in the porous heat sink fitted in a channel. The findings reveal that the effect of the inlet thermal boundary condition on the numerical calculations becomes weaker as the interstitial heat transfer coefficient increases. Criteria for local thermal equilibrium in various porous channels were also revealed.

Jiang et al. [16] performed numerical simulation on the forced convection heat transfer of water and air in plate channels filled with sintered bronze media using a local thermal non-equilibrium model with consideration of the wall effect caused by heat conduction in the plate wall and in the unheated section of the sintered porous media. The results showed that the lower value of wall porosity in sintered porous media as compared to the non-sintered packed beds helps to intensify convection heat transfer. In addition to this, the wall effect reduces the heat transfer coefficient near the front of the heated section and slightly increases it near the end of the heated section. Ould-Amer et al. [17] showed numerically that insertion of porous material between the heat generating blocks,

which were evenly mounted on a wall in a parallel plate channel, increases the mean Nusselt number up to 50% and reduces the maximum temperatures within the heated block as compared to the pure fluid case. Yang and Hwang [18] investigated turbulent fluid flow and heat transfer characteristics for a rectangular channel with porous baffles arranged on the top and bottom channel walls in periodically staggered way with air as working medium and using control volume-based finite difference method. Results showed that the porous-type baffles has lower friction factor than solid-type baffles and enhanced heat transfer relative to the smooth channel. Lage et al. [19] numerically studied a low permeability microporous heat sink for cooling phased-array radar systems. Their results suggested that an increased overall heat transfer coefficient could be obtained using such a heat sink which would reduce the operational temperature of the electronics for the same waste heat generation rate.

Forced convection heat and mass transfer inside the porous structures has also been studied experimentally using different material and fluid combinations. Jiang et al. [20] experimentally investigated forced convection heat transfer of water and air in sintered porous plate channels made of bronze particles sintered to a thin copper plate which was placed in the stainless steel channel. Heat load as high as 0.9 MW/m^2 was transferred at a pressure drop of 1.29 MPa/m with single phase water flow. In the study, the effects of fluid velocity, particle diameter of bronze material (d = 0.6, 1.2 and 1.7 mm), type of porous medium (sintered or non-sintered) and type of fluid (air or water) on the heat enhancement were examined. The results showed that convective heat transfer in the sintered porous plate channel was more intense than in the non-sintered porous plate channel, due to the reduced thermal contact resistance and the reduced porosity at the wall in the sintered channels. For the conditions in the study, the sintered porous medium enhanced the local heat transfer coefficient by 15 times for water and up to 30 times for air compared to the empty channel design. They also reported that the effective thermal conductivity of the sintered channels was much higher than that of the non-sintered media due to the improved thermal contact from the sintering process. In their study on a porous channel with sintered copper beads, Tzeng et al. [21] conducted experiments to study the effect of the bead particle size on the efficiency of heat exchange between the fluid and the solid phases for the heat sink. Three different test sections of sintered porous medium were made using copper beads of 0.71, 0.84 and 1.15 mm particle size, respectively. High pressure air was used as the cooling medium. It was reported that in the case of a smaller particle size, the overall wall temperature distribution is lower than that with the bigger particles for the same input heat flux due to the larger contact area involved with the smaller particle beads.

Heat transfer and pressure drop in a rectangular channel with sintered porous stainless steel inserts of different porosity were investigated experimentally by Hetsroni et al. [14] for the purpose of cooling mini-devices. Heat flux up to 6 MW/m^2 was removed by using a porous sample with 32% porosity and 20 μm average pore size. Under the experimental conditions, the difference between the wall and the inlet water temperatures did not exceed 55 K and the pressure drop was 4.5 bar. The authors also compared the efficiency of a sintered porous heat sink to an aluminum compressed foam heat sink and showed that the former provided very high heat transfer performance however it was accomplished by a drastic increase in pumping power. Jeigarnik et al. [22] examined convective heat transfer of water in flat plates and in channels filled with porous materials such as sintered spherical particles, nets, porous metal and felts. They found that the porous media increased the heat transfer coefficient 5–10 times although the hydraulic resistance increased even more.

Tzeng et al. [23] measured local and average heat transfer characteristics of asymmetrically heated sintered porous channels with metallic baffles. The fluid medium was air. Solid baffles were inserted periodically into the sintered metallic material in four modes – without baffles, with periodic baffles on the top portion, with periodic baffles on the bottom portion and with staggered periodic baffles on both sides. The study concluded that copper baffles helped to enhance the thermal conductivity through the solid matrix and promoted the heat transfer coefficient between the fluid and solid media. However, baffles also have some adverse effects that include reduction in the volume of the porous media (i.e. reducing the effective heat dissipation area) and preventing proper coolant flow into the regions around the neighboring baffles. In the study, the effect of bead diameter was also studied and it was seen that the heat transfer by forced convection in all modes increased as the bead diameter decreased.

In the present investigation, forced convection heat and mass transfer of water in a porous heat sink with sintered copper insert has been experimentally studied for the thermal control of the high-powered microprocessor. Sintered metal powder provides more efficient and compact heat transfer medium when compared to the metal foams or packed beds [14,20]. Copper and water are chosen as the appropriate combination for the present liquid cooling based system due to their superior heat transfer characteristics and chemical compatibility with each other. Amongst the heat transfer materials, copper can be considered as the most optimum choice for porous heat sink due to its high thermal conductivity (~400 W/m K), availability at reasonable cost in pure form, can be sintered from powder form and easy to machine. Regarding the coolant, the heat transfer capabilities of water are superior to those of air for the removal of high and concentrated heat fluxes, although with high hydraulic losses. In the view of the authors, there are not many references available in the literature that presents the performance of the sintered metal heat sink using copper–water combination. Hence, the present study will attempt to provide experimental results on the thermal and hydraulic performance of such system.

2. Description of the test prototype

Fig. 1(a) presents the design of the sintered porous heat sink that consists of the bottom portion or the cold plate, with the porous sample and flow arrangement, and the top portion, with the transparent cover plate and sealing flange. The bottom portion or lower housing consisted of a circular copper block of 50 mm diameter and 4 mm thickness. On the top face of the block, a rectangular section of 22 mm (L) × 20 mm (W) × 2 mm (D) was milled in which the porous insert of 14 mm (L) × 20 mm (W) × 2 mm (T) was sintered attached such that it occupied the entire cross section of the channel as shown in Fig. 1(b).

Sintered copper material that was manufactured using copper granules/powders of 100–200 mesh size was used as the porous medium in the heat sink prototype. Powder size dictates the pore size and pore distribution inside the porous structure. The Oxygen Free Copper (OFC) powders used in the porous sample have irregular rounded shaped particles that were sintered at a temperature slightly less than the melting point of copper in order to fuse and interlock the particles to form a porous matrix. Porosity and permeability are very important but contradictory parameters of the porous structure. High permeability and thus high porosity is advantageous for low hydraulic resistance whereas low porosity is desirable for high thermal conductivity of the porous sample. As a result, an optimum balance should be achieved between these properties from fluid flow and heat transfer point of view. The structural details of the sintered porous material are presented in

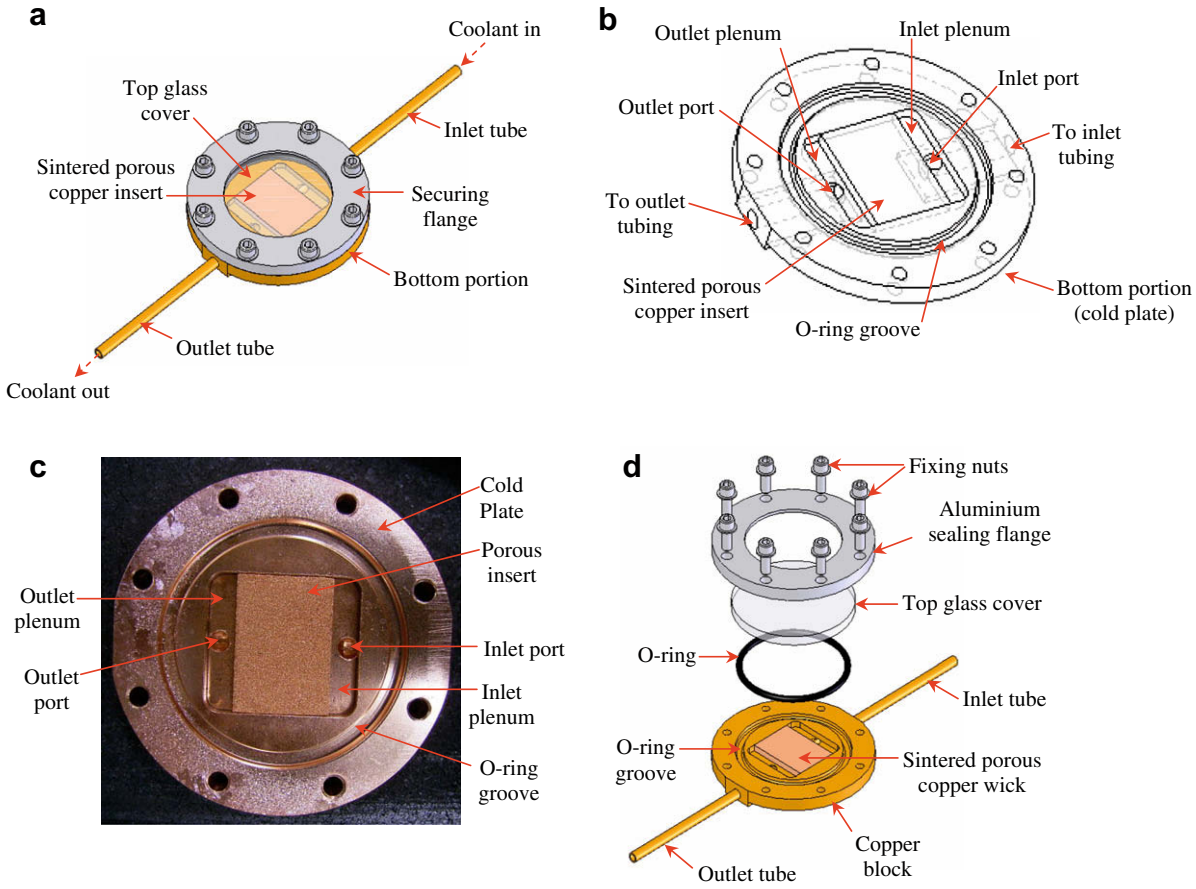

Fig. 1. Sintered porous heat sink. (a) Test prototype. (b) Internal details of the heat sink bottom portion. (c) Picture of the cooling section showing the porous copper media attached inside the rectangular channel. (d) Exploded view of the heat sink assembly showing different components.

Fig. 2 at different magnification scales that clearly show the copper particles fused together at the interfaces that support the superior thermal characteristics of the sintered porous structures as compared to the non-sintered ones.

Physical properties of a sintered copper porous media like permeability, porosity and maximum sample pore radius, as given in Table 1, were measured by simple experimental techniques explained in Singh et al. [24]. Permeability was determined from Darcy's law of fluid flow by using information on the measured volume flow rate through the cross section of the porous structure under constant pressure. For porosity two different methods: density method and soaking method were used. Density method calculates the porosity by weighing the porous samples and then comparing its density with the solid copper of same grade as copper powder whereas soaking method measures the density on the basis of volume of liquid soaked by the dry porous sample. The density method gave better results than the soaking method due to the problems of incomplete wetting or presence of close spaces and dead ends in the porous media. Pore radius was estimated from the U-tube bubble point testing method that equates the air pressure applied on one side of the porous sample to the interfacial surface tension forces between the porous structure and water on the other side.

Two holes were drilled at the diametrically opposite ends through the thickness of the circular copper block (or bottom section). These holes open into the inlet and outlet plenums located on either side of the porous insert. The inlet and outlet plenums helped in the evenly distribution and proper streaming of the coolant flow through the porous matrix. Fig. 1(c) shows the picture of the cold plate with the porous copper sample sintered attached inside the rectangular channel. Inlet and outlet tubes were soldered in the drilled holes to provide coolant flow through the porous insert. Fig. 1(d) presents the exploded view of the cooling section assembly showing the main components. The cold plate is enclosed from the top with a circular glass sheet which is kept in place with the help of a flange and nuts arrangement and provides a clear section for visualization. To avoid any bypass of the coolant along the contact surface, the top face of the porous insert should be perfectly flat and levelled with the glass cover. In the present model, a thin layer of Ethylene Propylene Diene Monomer (EPDM) rubber gasket (not shown in the Fig. 1) was also provided between the cold plate and top cover for channeling the coolant flow through volume of porous insert. In order to prevent any external leakage of the working fluid from the interface between the lower copper housing (bottom portion) and the top glass cover, a silicone O-ring seal was provided in the groove machined on the copper block. The active cooling area of the heat sink, i.e. portion available for the heat source attachment, corresponds to the cold plate footprint which is occupied by the porous material (14 mm (L) × 20 mm (W)). It is the area span by the coolant flow through the porous structure.

The coolant enters the heat sink via the inlet tube to the inlet plenum, passes through the porous structure where it absorbs the heat conducted from the source attached to the bottom of the cold plate. After absorbing heat from the porous medium by forced convection, the coolant exits the heat sink through the outlet plenum to the outlet tube. Fig. 3 presents the liquid flow path inside the porous heat sink.

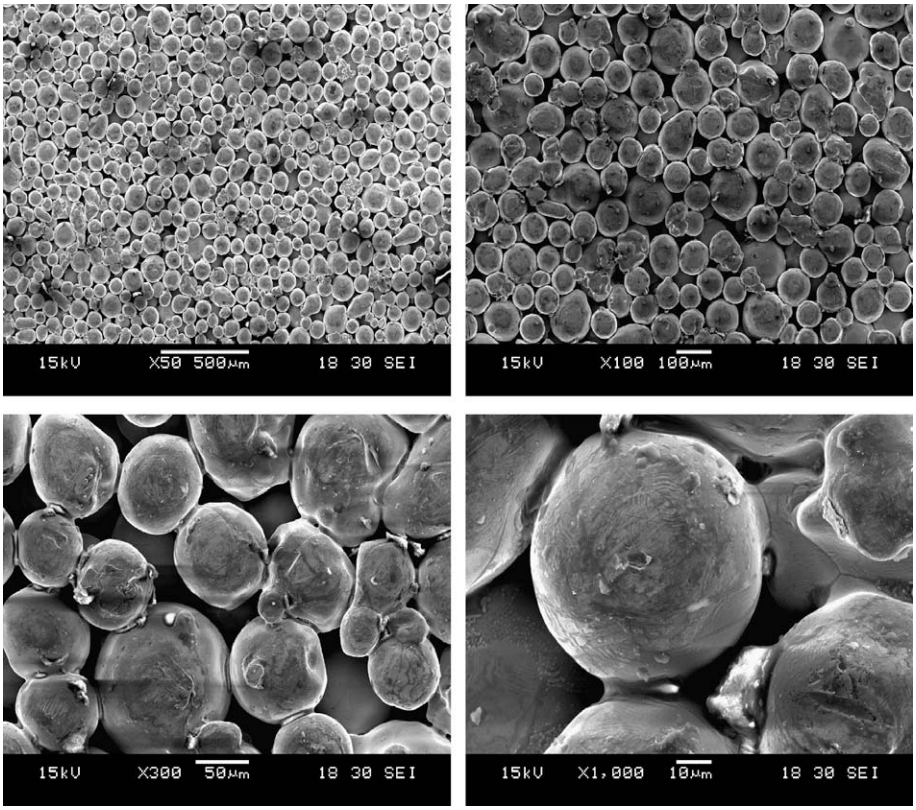

Fig. 2. Sample of the sintered copper porous material at different magnifications showing irregular copper particles fused together as a result of the sintering process.

Table 1
Flow properties of copper wick (100–200 mesh size).

Physical property	Value
Pore radius	<30 μm
Porosity	40%
Permeability	1.44×10^{-11} m^2

3. Experimental setup and test procedure

The experimental setup used to investigate forced convection heat transfer of water in sintered copper heat sink is shown schematically in Fig. 4. Thermal performance of the heat sink was tested under the condition of local heating of the porous heat sink using a heat source with thermal footprint of 7 mm x 7 mm (0.49 cm^2). In this case, heat load was applied on approximately 17.5% of the active cooling zone. The heat load simulator was fabricated from a copper block with two embedded cartridge heater rods. Heat generating block was symmetrically attached to the active zone at the bottom of the lower housing as depicted in Fig. 4. Heat losses from the source was minimized by means of thermal insulation provided by a bakelite plate attached to the heater base. The base plate also provided the required attachment pressure for the proper thermal contact between the heating face and the heat sink base. A layer of highly conductive thermal interface material was applied on the active area of heat sink base to reduce the thermal contact resistance.

The parameters measured in the experiment included the pressure at the inlet to the heat sink, mass flow rate of the coolant at outlet, applied heat load and temperatures at appropriate points. Eight T-type thermocouples were used to monitor temperature at different locations of the test prototype as shown in Fig. 5. To measure temperature at the junction of the heater and cold plate

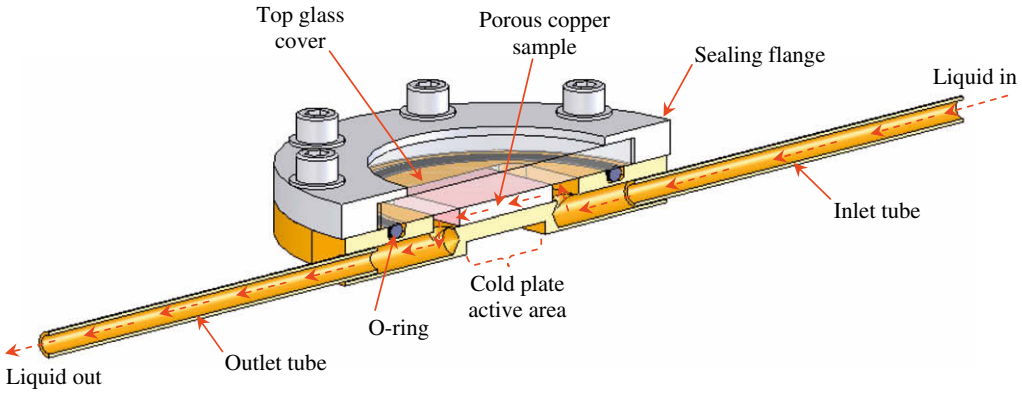

Fig. 3. Cross sectional view of the sintered porous heat sink showing the liquid flow pattern inside the cooling section.

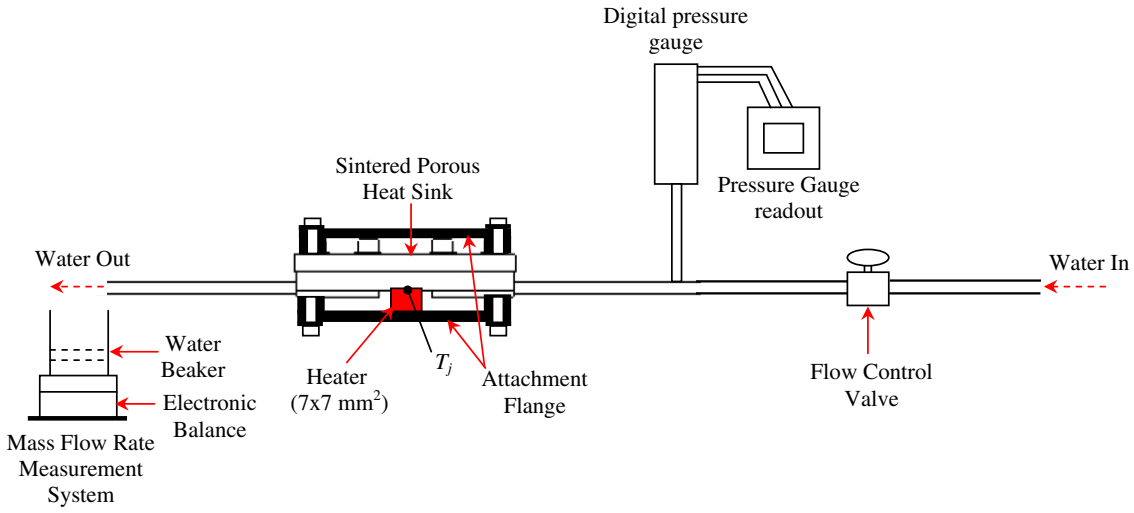

Fig. 4. Experimental setup for the sintered porous heat sink.

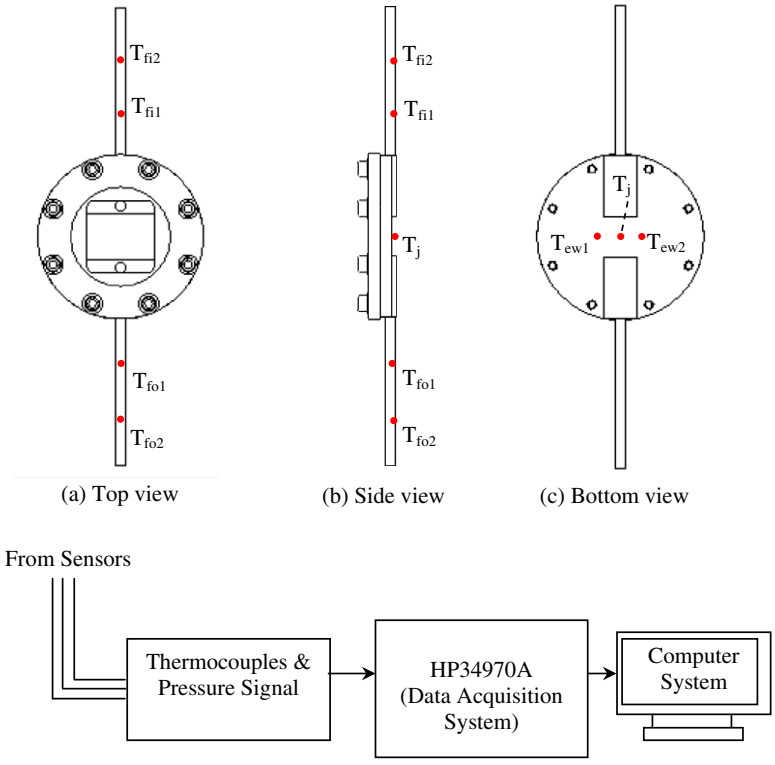

Fig. 5. Test setup for the sintered porous heat sink showing the locations of the thermocouple points.

(shown as T_j in Fig. 5), a thermocouple was fixed inside the groove machined in the center of the heater face using thermally conductive epoxy resin. The external surface temperature of the cold plate active zone was determined by taking the mean of readings from three thermocouples (T_j, T_{ew1} and T_{ew2}) attached to the lower housing. Two thermocouples were installed each at the inlet (T_{fi1} and T_{fi2}) and the outlet (T_{fo1} and T_{fo2}) of the heat sink to measure the coolant liquid entry and exit temperatures. To monitor and record the pressure and temperature readings during testing, an Agilent HP34970A data acquisition system was used. The mass flow rate of the coolant was measured by weighing the liquid flowing out of the heat sink in a given time interval using an electronic balance. To adjust and measure the input power to the heater, a digital power meter was used. All the tests were conducted with distilled water as the coolant.

For each experimental test on the porous heat sink, the input parameters, i.e. flow rate, input power and the inlet liquid temperature were fixed. All the temperature measurements were made at steady state conditions. Each experiment was run for several minutes until the fluid and thermal regimes inside the porous structure became stable. Steady state was assumed to occur when the fluctuations in the heat sink junction and wall temperatures were within ±1 °C. The experiments were carried out for the volume flow rates of 0.8–4.2 cm^3/s in the channel with the porous insert and heat load in the range of 10–150 W. In these tests, the inlet temperature of the liquid was maintained at 20 ± 2 °C.

4. Data reduction and uncertainty analysis

The measured data was utilised to conduct the hydraulic and thermal analysis on the forced convection through the sintered porous heat sink. For the hydraulic analysis, pressure drop through the porous structure and associated fluid pumping requirements to maintain junction temperature below maximum permissible limits for microprocessors were investigated. The thermal performance of the porous heat sink was assessed on the basis of the junction temperature (T_j), cold plate thermal resistance (R_{cp}) and overall heat transfer coefficient (h_o).

Heat losses from the exposed surfaces of the heat sink and the heater block were calculated from the energy balance between the power input to the heater and enthalpy rise of the coolant while passing through the heat sink. In these tests, convection and radiation heat losses were estimated to be 5–10% of the applied heat load. It should be noted that heat exchange with the ambient shows a strong dependence on the temperature difference between hot surfaces and ambient. At very low heat loads (<10 W), there was heat gain from the atmosphere due to lower coolant temperature. However, over most range of the applied heat, there were heat losses to the ambient that magnifies with increase in the input power to the heater.

The thermal resistance of the cold plate (R_{cp}) was calculated on the basis of the junction temperature (T_j) and the fluid mean temperature (T_{fm}) as follow:

$$R_{cp} = \frac{(T_j - T_{fm})}{Q_h^{\bullet}} \tag{1}$$

The overall heat transfer coefficient (h_0) from cold plate external wall to liquid coolant is defined as:

$$h_o = \frac{Q_h^{\bullet}}{A_p(T_{ew} - T_{fm})} \tag{2}$$

where $Q_h^{\bullet}$ is the heat load applied to the active area of the porous heat sink, A_p is the planar area of porous insert footprint inside the channel, T_{ew} is the mean temperature of the cold plate external wall determined from the average of three thermocouple attached to the heat sink base (T_j, T_{ew1} and T_{ew2}) and T_{fm} is the mean fluid temperature calculated on the basis of the inlet and the outlet temperatures of the liquid in the test section. Fig. 6 shows the relevant heat transfer areas with respect to the thermocouples locations.

Input heat load was measured by taking the product of the voltage and current readings from the wattmeter. The error in heat load measurement was high at low input power. In this case, the maximum uncertainty of ±2.26% was recorded. The mass flow rate of water ($m^{\bullet}$) was controlled by flow control valve and was measured by simple weighing method with an uncertainty of ±0.24%. Thermal properties of the fluid were determined at the mean coolant temperature by using fifth degree polynomials [6] that were obtained by curve fitting of the relevant properties with respect to the temperature. Maximum error involved in this case was less than ±3%. Uncertainty in the measurement of heat transfer areas was within ±2.1%. Temperatures at the inlet, outlet and wall of the heat sink were measured by T-type thermocouples calibrated using a constant temperature bath with an accuracy of ±0.1 °C. The error in determining the convection heat transfer coefficient (h_o), according to Eq. (2), is due to the uncertainty associated with the measurement of input heat load ($Q_h^{\bullet}$), heat transfer area (A_p) and difference between the average external wall and mean liquid temperatures ($T_{ew} - T_{fm}$). It should be noted that the uncertainty related to h_o is higher at low heat loads and for high mass low rate of the coolant due to the smaller rise in the liquid temperature through the test section. As a result, the maximum error for heat transfer coefficient as determined at these conditions was

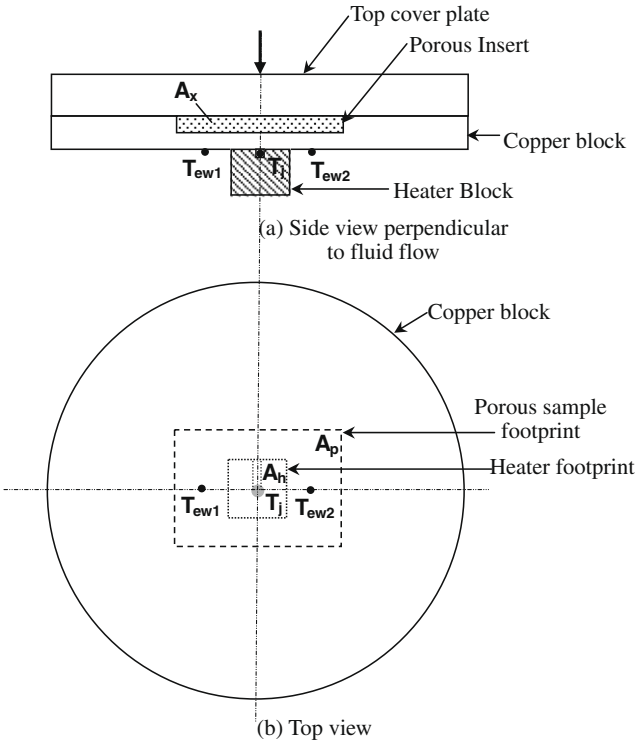

Fig. 6. Cross sectional views of the sintered porous heat sink prototype presenting details on the heat transfer areas and associated locations of temperature measurement points.

±12.2%. For the hydraulic diameter of the channel and thermal conductivity of the water at the mean coolant temperature, the uncertainties of ±2.2% and ±0.5%, respectively, were calculated which provide estimate of ±11.4% on the Nusselt number. For the cold plate thermal resistance (R_{cp}), the uncertainty was estimated to be ±10%.

Pressure drop across the porous insert was measured using a pressure transducer with an uncertainty of 0.25% of the full scale range of 1 MPa. Experimental uncertainty for the permeability was estimated from the errors associated with the measurement of mass flow rate, pressure drop, fluid properties and linear dimensions, and was within ±6.49%. Porosity of the copper insert was measured by density method with an uncertainty of 2.1%. In the determination of the effective thermal conductivity of the water saturated copper wick from Fourier's law, the experimental uncertainty was less than ±6%.

5. Experimental results and discussion

5.1. Pressure drop analysis

Fig. 7(a) shows the pressure drop through the sintered porous matrix as a function of the volume flow rate of the coolant. It is noted from the plot that flow through the porous matrix requires very high inlet pressure for the liquid due to high frictional losses inside the bulk of porous structure. These pressure losses are attributed to the large contact area between the liquid and the porous structure, and tortuous flow path that the liquid encounters while passing through the porous matrix. Pressure drop across the porous structure (ΔP_p) can be expressed by Darcy law [25] as:

$$\Delta P_p = \frac{V^{\bullet}\mu_l t_p}{A_x k_p} \tag{3}$$

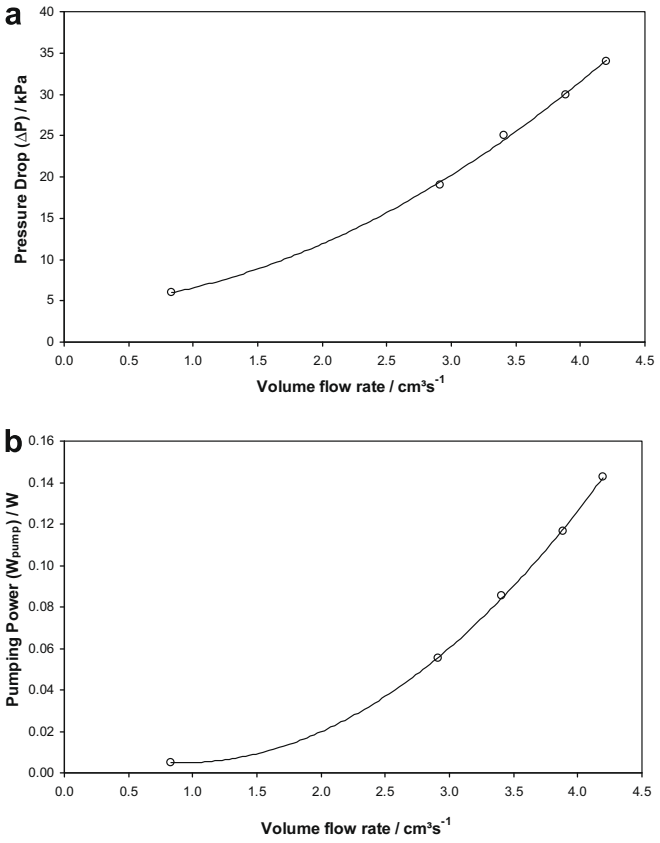

Fig. 7. Effect of volume flow rate on the (a) pressure drop across the porous insert and (b) pumping power.

where k_p is the specific permeability of the porous medium, A_x is the cross sectional area of the porous insert perpendicular to the flow direction as shown in Fig. 6.

For the test sample, the permeability ($\sim 1.44 \times 10^{-11}$ m^2) and pore radius (<30 μm) values are quite low that increases the hydraulic losses substantially. The high flow resistance encountered inside the porous structure increases the requirements on the mechanical power required to push the liquid through the porous volume. Pumping power (W_{pump}) is given by the product of the pressure drop across the porous insert (ΔP_p) and the volumetric flow rate of the liquid ($V^\bullet$) through the test prototype.

$$W_{pump} = \Delta P_p V^\bullet \quad (4)$$

Fig. 7(b) presents the pumping power required to maintain the required coolant flow through the porous sample. It should be noted that power prerequisites for the sintered porous structure is greater than the non-sintered porous beds and metal foams due to their low porosity and thus high flow resistances. However, the high pumping requirements for sintered porous heat sink is counterbalance by the superior thermal characteristics of these heat sinks owing to their high effective thermal conductivity.

5.2. Heat transfer analysis

5.2.1. Junction temperature

Heat load dependence of the junction temperature for different volume flow rates in the range of 0.8–4.2 cm^3/s is shown in Fig. 8. For a particular flow rate, the junction temperature presented a monotonic rise with the increase in the applied heat load. It is noted from the plot that the rate of junction temperature rise with increasing heat load is dependent on the coolant flow rate. For

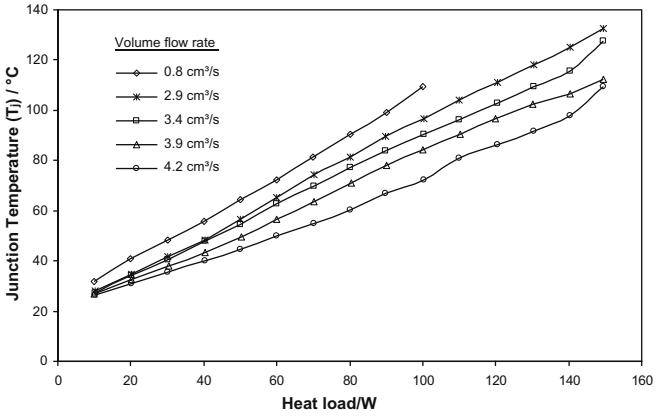

Fig. 8. Heat load dependence of the junction temperature at different coolant flow rates.

0.8 cm^3/s, the junction temperature rise at the rate of ~0.8 °C/W whereas the rise was limited to ~0.55 °C/W at 4.2 cm^3/s of coolant flow rate. This improvement in the thermal performance of the heat sink is made possible by the convective heat transfer augmentation inside the bulk of the porous structure at high flow rates. Looking at thermal trends for different flow rates, it is observed that for the fixed input power there is a drop in junction temperature with rising fluid flow rate. At 100 W, increase in coolant flow from 0.8 to 4.2 cm^3/s results in drop of 36.9 °C at the heater-cold plate junction. It is further noted that the effect of the flow rates on the steady state junction temperature is increasingly distinct at high heat loads. This is due to the fact that at low heat loads, heat dissipation to ambient by spreading through cold plate base which is made from high conductive copper material is sufficient to cool the heat source. In electronic cooling, generally the maximum safe working temperature for microprocessors is limited to 100 ± 5 °C. The present design of the microporous heat sink was able to transfer heat flux as high as 2.9 MW/m^2 (at 4.2 cm^3/s and 140 W) while maintaining the junction temperature below 100 °C limit. In this study, the sink was not tested for flow rates beyond 4.2 cm^3/s due to the limitation on the maximum available water supply pressure at the inlet of the cooling section.

5.2.2. Thermal resistances

Fig. 9 shows the variation of temperatures with applied heat load at different locations of the heat sink for 4.2 cm^3/s of coolant flow through the porous channel. In the plot, heat sink internal

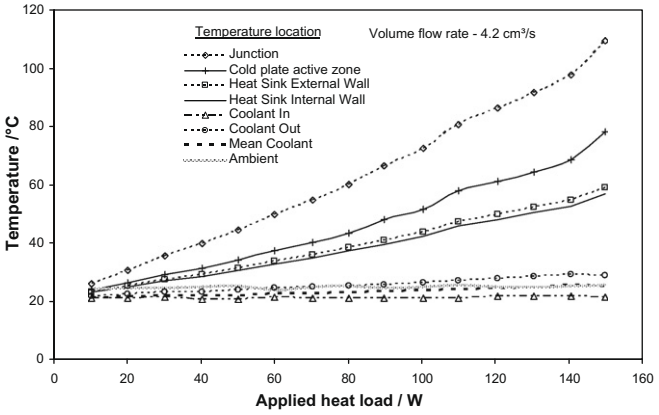

Fig. 9. Relationship between the temperature and the applied heat load for different locations in the sintered porous heat sink.

wall temperature (T_{iw}) is estimated from the external wall temperature (T_{ew}) by using Fourier law of heat conduction as given below:

$$T_{iw} = T_{ew} - \frac{Q''_h t_b}{k_{cu} A_p} \quad (5)$$

The cold plate active zone temperature (T_{az}) as represented in Fig. 10 is calculated from Eq. (6) by using information on the junction temperature (T_j) and contact resistance (R_{ct}) of the thermal interface material used at the heater-cold plate interface.

$$T_{az} = T_j - Q''_h R_{ct} \quad (6)$$

$$\text{where } R_{ct} = \frac{t_{TIM}}{k_{TIM} A_h} \quad (7)$$

In the present case, thermally conductive silicon grease was used as the thermal interface material (also called as TIM). Considering perfectly smooth mating surfaces and assuming thermal conductivity of 5 W/m K and bold line thickness (or TIM thickness) of 2 mils (1 mil = 0.0254 mm) for the thermal interface material [26], the contact resistance is approximated as 0.21 °C/W.

As shown in the Fig. 9, the temperatures showed continuous rising trend with the increase in the heat load except liquid inlet temperature which was the controlled parameter in the experiment. For a particular heat load, the temperature difference between any two points on the graph represents the thermal resistance between the associated locations of the heat sink. In other words, the thermal resistances between different components of the cold plate can be quantified from Fig. 9 and regions that offer high thermal resistances to the heat flow can be identified.

Fig. 10 presents the thermal circuit diagram to characterize different thermal resistances in the porous metal heat sink. Starting from heater active face at junction temperature (T_j), the thermal resistance is imposed at the contact between the heater footprint and the cold plate active zone (known as contact or interface resistance, R_{ct}) due to the low heat conductance of the interface material. Next, the conductive resistance (known as spreading resistance, R_{sp}) is offered to the thermal spreading from the local heated portion of the cold plate (equal to heater area, i.e. 7×7 mm^2) to its heat dissipation area (equal to area of porous insert, i.e. 14×20 mm^2, considering negligible heat losses to ambient). Further, the heat flows through the thickness of the cold plate where it incurs conduction resistance through the wall (R_w) and then eventually it is convected to the coolant via sintered porous insert where it underwent convective resistance (R_{conv}).

On the basis of Fig. 9, the graph is plotted in Fig. 11(a) to quantify the main components of the cold plate resistance. It is evident from the graph that R_{ct} proved to be the main component and contributed to approximately 44% of the cold plate thermal resistance. R_{ct} depends on number of factors including type of thermal interface material used [26], contact pressure and surface flatness. In the designed heat sink, superior heat transfer characteristics were achieved from the cold plate heated wall to the coolant by forced convection of water through the sintered copper structure which is apparent from the low heat convective resistance. Over the range of applied heat load and coolant flow rate of 4.2 cm^3/s, the convective resistance was around 0.18 °C/W and makes up 37% of the cold plate thermal resistance. It should be noted that sintered copper and water provide an efficient heat transfer system due to their high thermal conductivities (~400 W/m K for copper material and 0.6 W/m K for water) that helps to reduce the convection heat flow resistance. As the heat sink body was made from high conductive copper material, the spreading resistance and cold plate wall resistance was only 0.075 °C/W (16% of R_{cp}) and 0.015 °C/W (3% of R_{cp}), respectively. It should be noted that both wall and spreading resistance is the direct consequence of the thermal dispersion through the heat sink base plate. In the present discussion, these resistances are differentiated as per the temperature measurement locations shown in Fig. 10.

Fig. 11(b) is plotted to study the variation of the cold plate thermal resistance with respect to the Reynolds number (Re) calculated on the basis of the hydraulic diameter of the flow channel. It is noted that rate of change of R_{cp} at high Reynolds number is more drastic as compared to the low Reynolds number flow. As an example, change in Re from 289 to 331 produces a corresponding decrease of 0.06 °C/W in R_{cp} whereas Re increase from 374 to 408 results in 0.13 °C/W drop in R_{cp}, which is more than double of the previous case. Such behaviour in porous structures can be attributed to the relative magnitude of the viscous and the inertial forces associated with the fluid flowing through the micro pores. At low Reynolds number, the pressure losses due to the relative high viscosity of water can dominate the inertial or pumping force pushing the fluid. As a result, coolant is not properly channeled through the bulk of the porous matrix. With the increase in the flow pressure, the coolant is uniformly filtered through the porous volume thereby enhancing the heat exchange process between the coolant and porous media.

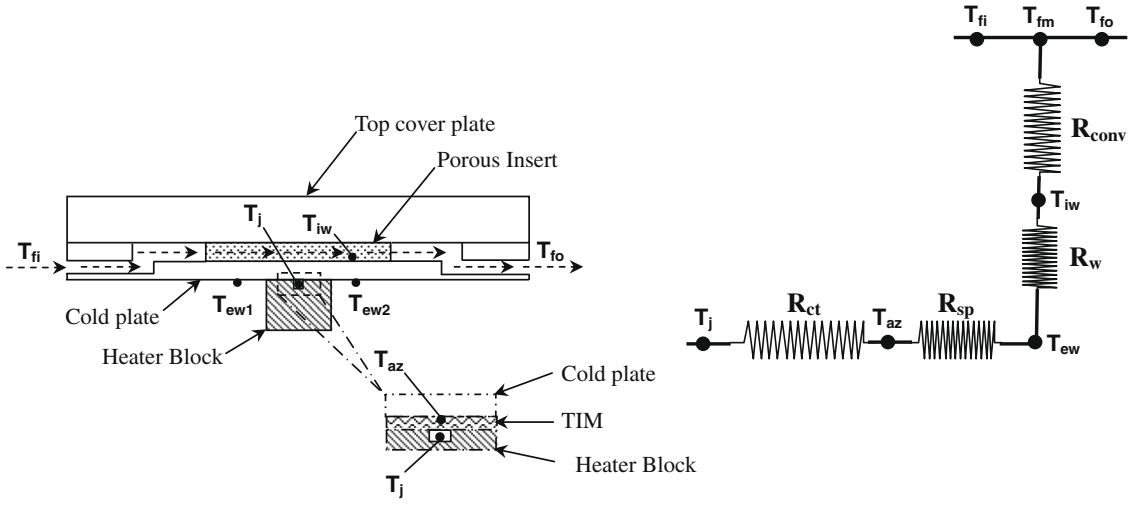

(a) Sectional Side view parallel to fluid flow

(b) Thermal circuit diagram

Fig. 10. Different components of the cold plate thermal resistance and the related temperature measurement points.

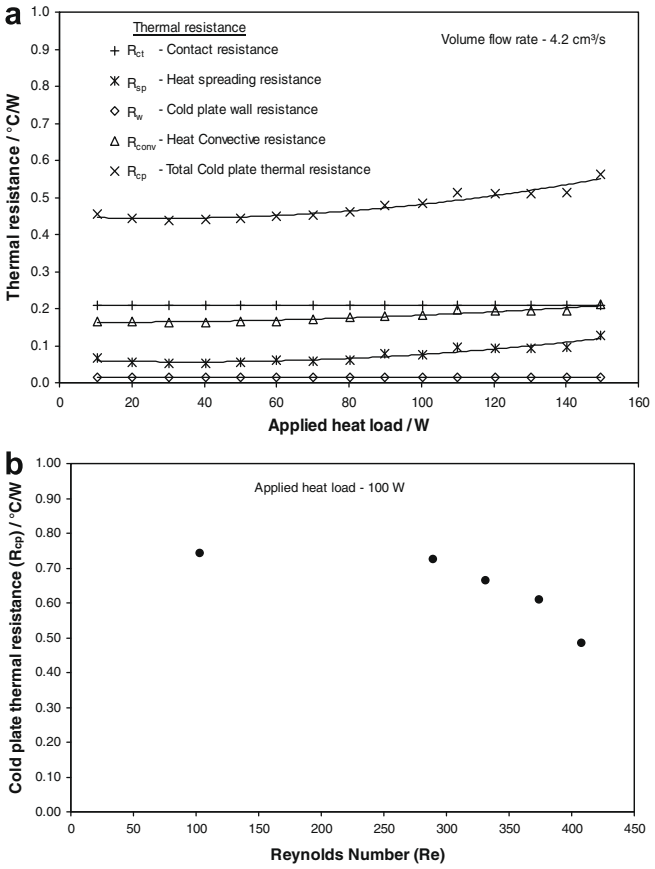

Fig. 11. (a) Thermal resistances for different components of the cold plate design. (b) Cold plate thermal resistance versus Reynolds number at input heat load of 100 W.

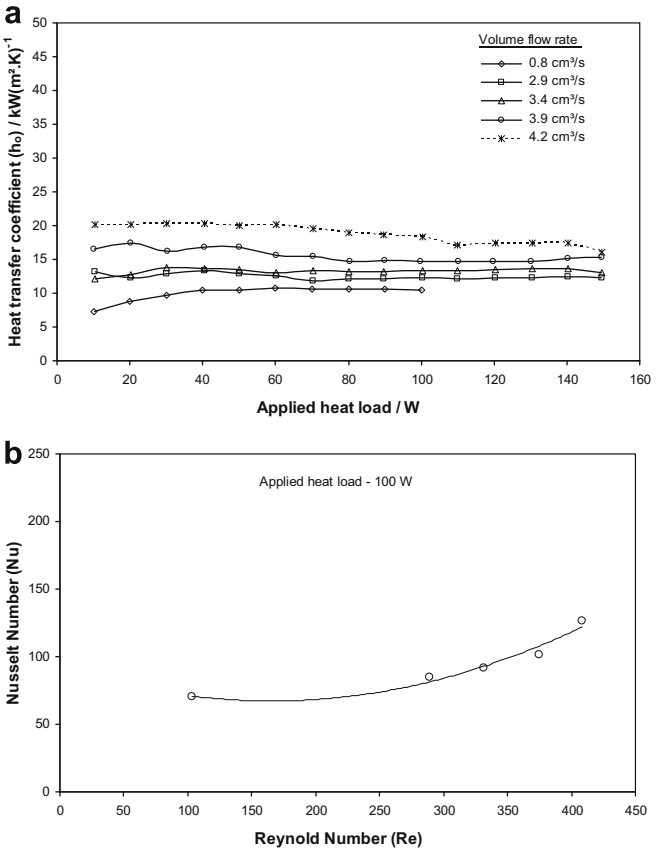

Fig. 12. (a) Heat transfer coefficient versus applied heat load for different coolant flow rate through the porous structure. (b) Relation between Nusselt number and Reynolds number for the sintered porous heat sink at the input heat load of 100 W.

5.2.3. Heat transfer coefficient

Fig. 12(a) shows the distribution of the overall heat transfer coefficient (h_o) from cold plate external wall to the coolant for different volume rates. The heat transfer coefficient enhanced with the increase in the flow rate and achieves a maximum value of 20,000 W/m^2 K at 4.2 cm^3/s. Such a high heat transfer coefficient for porous channel is an order of magnitude greater than the empty channel and supports the superior heat transfer augmentation characteristics of the sintered porous heat sink. For the given flow rate, the value of h_o remained nearly constant with the change in the applied heat load due to the stable flow characteristics and thus constant thermal resistance. The relation between the Nusselt number (Nu) and Reynolds number (Re) based on the channel hydraulic diameter is shown in Fig. 12(b). Maximum value of 126 for Nu was achieved at highest Re of 408.

5.2.4. Effective thermal conductivity

The effective thermal conductivity of the sintered porous media is very critical design parameter and decides the overall heat transfer effectiveness of the porous heat sink. In the sintered porous structure high effective thermal conductivity is achievable as compared to the non-sintered porous media due to better thermal contact between the powder particles and also between particles and wall through sintering process. A simple experiment based on the unidirectional conduction heat transfer was conducted to determine the effective thermal conductivity of the sintered copper wick saturated with water.

The test setup consisted of a sealed rectangular copper container with water saturated sintered copper structure, 40% porous, such that bottom face of the sample is provided with uniform heat flux while the top face is cooled using fin heat exchanger with air flow arrangement. Results obtained from the experiment were substituted in Eq. (8) which estimated the effective thermal conductivity of water saturated copper porous media as 32 W/m K.

$$k_e = \frac{Q_a^{\bullet} t_s}{(T_{bf} - T_{tf}) A_s} \tag{8}$$

The experimentally obtained effective thermal conductivity is compared to the values predicted from the volumetric averaging approach [27] as per Eq. (9) and from the correlation suggested by Alexander [28] as given by Eq. (10).

$$k_e = k_p(1-\varepsilon) + \varepsilon k_l \tag{9}$$

$$k_e = k_l \left(\frac{k_l}{k_p}\right)^{-(1-\varepsilon)^{\alpha}} \tag{10}$$

The effective thermal conductivity of the sintered copper media predicted by the volume averaging technique is as high as 240.27 W/m K which is more than seven times of the experimental data (32 W/m K). However, the Alexander correlation is able to provide better approximation (76.12 W/m K) than the volume averaging equation. It should be noted that calculated effective thermal conductivity from Eq. (10) is very sensitive to the porosity of the test sample. For example, change in porosity by 15% can alter the effective conductivity by two times. As a result, more precise testing is needed to minimize experimental errors and get better match between theory and experiment.

Due to the high thermal conductance of the copper material, the effective thermal conductivity of sintered copper porous media (~32 W/m K) is quite high when compared to the sintered bronze

porous media (~3.4 W/m K) as obtained experimentally by Jiang et al. [20]. This helps to classify the copper based sintered porous structures as a competitive candidate for the porous heat sink with high heat transfer characteristics.

6. Conclusions

The outcomes of the study can be summarized as follows:

- A sintered porous heat sink with porous copper channel and distilled water as the coolant was investigated experimentally for cooling of high-powered microprocessors for servers.
- With the designed prototype, heat flux up to 2.9 MW/m^2 was removed by porous copper insert with 40% porous volume and 1.44×10^{-11} m^2 permeability, while maintaining the junction temperature below the maximum permissible limit of 100 ± 5 °C.
- At maximum Re of 408 and heat load of 150 W, the sintered porous heat sink showed best thermal performance with minimum value of 0.48 °C/W for cold plate thermal resistance and maximum values of 20 kW/m^2 K and 126 for heat transfer coefficient and Nusselt number, respectively.
- Detailed analysis on different components of cold plate thermal resistance reveals that contact resistance is the major component and makes up 44%, while convection resistance accounts for 37% of the R_{cp}.
- With sintered copper based porous heat sink, high convective heat transfer between the fluid and the porous matrix was achieved due to the high effective thermal conductivity of sintered porous copper (~32 W/m K).
- Forced convection heat transfer through the porous structure is accompanied by high pressure drop for coolant which was 34 kPa at maximum flow rate of 4.2 cm^3/s. As a result, the use of the sintered porous heat sink should be intended for high-end electronics like servers in data center where power is available to fulfill the pumping requirements.

References

[1] R.R. Schmidt, E.E. Crus, M.K. Lyengar, Challenges of data center thermal management, IBM Journal of Research and Development 49 (4/5) (2005) 709–723.

[2] D.B. Baer, Emerging cooling requirements and systems in telecommunications spaces, in: Proceedings of the Twenty-Third International Telecommunications Energy Conference, IEEE, New York, 2001, pp. 95–100.

[3] K.G. Brill, 2005–2010 Heat density trends in data processing, computer systems, and telecommunications equipments: perspectives, implications, and the current reality in many data centers, White paper, The Uptime Institute Inc., Version 2.0, New York, USA, 2005, pp. 1–16.

[4] C.D. Patel, R. Sharma, C.E. Bash, A. Beitelmal, Thermal consideration in cooling large scale high compute density data centers, in: Proceedings of the Eighty Intersociety Conference on Thermal and Thermomechanical Phenomena in Electronic Systems, IEEE, 2002, pp. 767–776.

[5] L. Stahl, C. Belady, Designing an alternative to conventional room cooling, in: Proceedings of the Twenty-Third International Telecommunications Energy Conference, IEEE, 2001, pp. 109–115.

[6] R. Singh, Thermal control of high-powered desktop and laptop microprocessors using two-phase and single-phase loop cooling systems, Ph.D. thesis, RMIT University, Melbourne, Australia, 2006.

[7] V.V. Calmidi, R.L. Mahajan, Forced convection in high porosity metal foams, Journal of Heat Transfer 122 (3) (2000) 557–565.

[8] H.L. Fu, K.C. Leong, X.Y. Huang, C.Y. Liu, An experimental study of heat transfer of a porous channel subjected to oscillating flow, Journal of Heat Transfer 123 (1) (2001) 163–170.

[9] L. Tadrist, M. Miscevic, O. Rahli, F. Topin, About the use of fibrous materials in compact heat exchangers, Experimental Thermal and Fluid Science 28 (2) (2004) 193–199.

[10] C. Cui, X.Y. Huang, C.Y. Liu, Forced convection in a porous channel with discrete heat sources, Journal of Heat Transfer 123 (2) (2001) 404–407.

[11] W.H. Hsieh, J.Y. Wu, W.H. Shih, W.C. Chiu, Experimental investigation of heat-transfer characteristics of aluminum–foam heat sinks, International Journal of Heat and Mass Transfer 47 (23) (2004) 5149–5157.

[12] Y.C. Lee, W. Zhang, H. Xie, R.L. Mahajan, Cooling of a FCHIP package with 100 W 1 cm^2 chip, Proceedings of the 1993 ASME International Electronic Package Conference, vol. 1, ASME, NY, USA, 1993, pp. 419–423.

[13] C.H. Chao, J.M. Li, Foam–metal heat sinks for thermal enhanced BGA package applications, in: The Eleventh International Symposium on Transport Phenomena ISTP-II, vol. 4, Hsinchu, Taiwan, pp. 23–29.

[14] G. Hetsroni, M. Gurevich, R. Rozenblit, Sintered porous medium heat sink for cooling of high-power mini-devices, International Journal of Heat and Fluid Flow 27 (2) (2005) 259–266.

[15] T.M. Jeng, S.C. Tzeng, Y.H. Hung, An analytical study of local thermal equilibrium in porous heat sinks using fin theory, International Journal of Heat and Mass Transfer 49 (11–12) (2006) 1907–1914.

[16] P.X. Jiang, M. Li, Y.C. Ma, Z.P. Ren, Boundary conditions and wall effect for forced convection heat transfer in sintered porous plate channels, International Journal of Heat and Mass Transfer 47 (10–11) (2004) 2073–2083.

[17] Y. Ould-Amer, S. Chikh, K. Bouhadef, G. Lauriat, Forced convection cooling enhancement by use of porous materials, International Journal of Heat and Fluid Flow 19 (3) (1998) 251–258.

[18] Y.T. Yang, C.Z. Hwang, Calculation of turbulent flow and heat transfer in a porous-baffled channel, International Journal of Heat and Mass Transfer 46 (5) (2003) 771–780.

[19] J.L. Lage, A.K. Weinert, D.C. Price, R.M. Weber, Numerical study of a low permeability microporous heat sink for cooling phased-array radar systems, International Journal of Heat Mass Transfer 39 (17) (1996) 3633–3647.

[20] P.X. Jiang, L. Meng, T.J. Lu, L. Yu, Z.P. Ren, Experimental Research on convection heat transfer in sintered porous plate channels, International Journal of Heat and Mass Transfer 47 (10–11) (2004) 2085–2096.

[21] S.C. Tzeng, W.Y. Jywe, C.W. Lin, Y.C. Wang, Mixed convection heat-transfers in a porous channel with sintered copper beads, Applied Energy 81 (1) (2005) 19–31.

[22] U.A. Jeigarnik, F.P. Ivanov, N.P. Ikranikov, Experimental data on heat transfer and hydraulic resistance in unregulated porous structures, Teploenergetika 2 (1991) 33–38. in Russian.

[23] S.C. Tzeng, T.M. Jeng, Y.C. Wang, Experimental study of forced convection in asymmetrically heated sintered porous channels with/without periodic baffles, International Journal of Heat and Mass Transfer 49 (1–2) (2006) 78–88.

[24] R. Singh, A. Akbarzadeh, C. Dixon, M. Mochizuki, Experimental determination of the physical properties of a porous plastic wick useful for capillary pumped loop applications, in: Proceedings of the 13th International Heat Pipe Conference, Preprint, vol. 2, Shanghai, China, 2004, pp. 139–145.

[25] A.E. Scheidegger, The Physics of Flow through Porous Media, University of Toronto Press, Great Britain, 1974.

[26] E.C. Samson, S.V. Machiroutu, J.Y. Chang, I. Santos, J. Hermerding, A. Dani, R. Prasher, D.W. Song, Interface material selection and a thermal management technique in second-generation platforms built on Intel® Centrino™ mobile technology, Intel Technology Journal 9 (1) (2005) 75–86.

[27] P.D. Dunn, D.A. Reay, Heat Pipes, Pergamon Press, Great Britain, 1994.

[28] E.G. Alexander, Structure–property relationships in heat pipe wicking materials, Ph.D. thesis, North Carolina State University, NC, USA, 1972.